

1992

## A Moving Optical Fibre Technique for Structure Analysis of Heterogenous Products: Application to the Determination of the Bubble-Size Distribution in Liquid Foams

C. G. J. Bisperink

J. C. Akkerman

A. Prins

A. D. Ronteltap

Follow this and additional works at: <https://digitalcommons.usu.edu/foodmicrostructure>



Part of the [Food Science Commons](#)

---

### Recommended Citation

Bisperink, C. G. J.; Akkerman, J. C.; Prins, A.; and Ronteltap, A. D. (1992) "A Moving Optical Fibre Technique for Structure Analysis of Heterogenous Products: Application to the Determination of the Bubble-Size Distribution in Liquid Foams," *Food Structure*: Vol. 11 : No. 2 , Article 2.

Available at: <https://digitalcommons.usu.edu/foodmicrostructure/vol11/iss2/2>

This Article is brought to you for free and open access by the Western Dairy Center at DigitalCommons@USU. It has been accepted for inclusion in Food Structure by an authorized administrator of DigitalCommons@USU. For more information, please contact [digitalcommons@usu.edu](mailto:digitalcommons@usu.edu).



A MOVING OPTICAL FIBRE TECHNIQUE FOR STRUCTURE ANALYSIS OF  
HETEROGENEOUS PRODUCTS: APPLICATION TO THE DETERMINATION OF THE  
BUBBLE-SIZE DISTRIBUTION IN LIQUID FOAMS

C.G.J. Bisperink\*, J.C. Akkerman, A. Prins and A.D. Ronteltap

Department of Dairy Science & Food Physics  
Agricultural University Wageningen  
The Netherlands

**Abstract**

The bubble-size distribution in liquid foams measured as a function of time can be used to distinguish between the physical processes that determine the breakdown of foams. A new method based on an optical fibre technique was developed to measure various foam characteristics e.g. the rate of drainage, the rate of foam collapse, the change in gas fraction, interbubble gas diffusion (disproportionation) and the evolution of the bubble-size distribution during the ageing of the foam. The method consists of an optical sensor that can distinguish between phases with distinct refractive indexes as are found in liquid foams.

**Introduction**

Foams are basically unstable, meaning that foam properties vary with time as a result of shifts in the spatial distribution of gas and liquid in the foam. The three main physical processes that contribute to the instability of foams are drainage, coalescence and disproportionation.

Drainage is the liquid flow from a foam caused by gravity and capillary forces resulting in a dryer foam in which the bubbles may become distorted. Coalescence is the merge of two bubbles as a result of the rupture of the film between the bubbles. Larger bubbles appear and the number of bubbles decreases. Disproportionation is interbubble gas diffusion resulting in growth of the larger bubbles and shrinkage of the smaller bubbles that may finally disappear.

These three processes affect the distribution of the liquid and gas phase in the foam and thus alter the foam properties (Ronteltap 1989). A new method called the Foam Analyzer was developed to measure various foam characteristics (Ronteltap et al. 1989). Since then, the apparatus has undergone great improvements. As a result of automation of the method, the resolution is increased, the time needed for the calculation of the bubble-size distribution was reduced to 1 minute, making it possible to do measurements every minute and the method, including foam production, was completely standardized. Therefore the properties of the liquid used for foam production determine the characteristics of the initial foam column. Furthermore the technique to produce the hemispherical tip at the end of the glass fibre was improved. It is possible now to measure the rate of drainage, the rate of foam collapse, changes in the gas fraction and the foam height and the evolution of the bubble-size distribution simultaneously in one sample as a function of time.

---

Initial paper received December 13, 1991  
Manuscript received April 2, 1992  
Direct inquiries to C.G.J. Bisperink  
Telephone number: (+31) 8370 82520  
Fax number: (+31) 8370 83669

---

**Key Words:** Foams, physical stability, bubble-size distribution, drainage, disproportionation, coalescence, optical fibre.

\*Address for correspondence:

Department of Dairy Science & Food Physics  
Agricultural University Wageningen  
Bomenweg 2, 6703 HD Wageningen  
The Netherlands.

Phone No.: (+31).8370.82520  
Fax No. : (+31).8370.83669

**Principle and performance of the technique**

In the Foam Analyzer (a schematic drawing is presented in figure 1) a mechanical part is used to move the glass fibre downwards through a foam at known speed in such a way that the position of the glass fibre sensor is known as a function of time. An opto-electronic part that consists of the optical glass fibre sensor and electronic equipment is used for signal conversion, data-acquisition and data processing. From the opto-electronic unit,

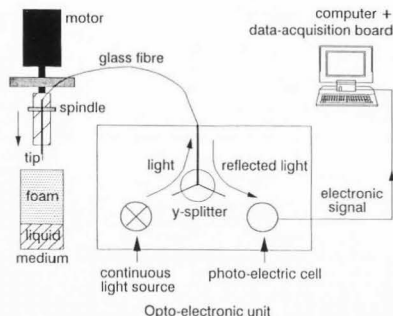


Figure 1: A schematic representation of the Foam Analyzer.

light is sent into the fibre. At the end of the fibre, the amount of light reflected depends on the optical properties of the surrounding medium. The reflection of the light in the end of the sensor is discussed first by Frijlink (1987) and later by Akkerman et al. (1991). They explain that the amount of reflected light depends to a large extent on the difference between the refractive index of the glass and the refractive index of the medium surrounding the sensor. Therefore, the two phases in foam, i.e. liquid and gas, can be distinguished by moving the glass fibre sensor through the foam.

By doing measurements in a system that consists of several horizontal films at known distances in a capillary tube the necessary frequency of sampling was determined. It became clear that at a sensor speed of  $10 \text{ cm s}^{-1}$ , the sampling frequency had to be at least  $100 \text{ kHz}$  in order to get accurate results. At lower sampling frequencies, not all the films were detected when they became thin as a result of drainage and evaporation.

Experiments were done in which the gas fractions were calculated independently in two different ways in order to get information about the relation between the accuracy of the method and the sampling rate and sensor speed. In one way the gas fraction was calculated with equation 1.

$$\Phi_g = \frac{(H_{11} - H_f)}{(H_{12} - H_f)} \quad (1)$$

where  $\Phi_g$  = The gas fraction in the foam [-].

- $H_{11}$  = The distance from the starting position of the glass fibre sensor to the liquid surface before a foam column is produced [m].
- $H_f$  = The distance from the starting position of the glass fibre sensor to the foam surface [m].
- $H_{12}$  = The distance from the starting position of the glass fibre sensor to the liquid-foam interface [m].

In the second way the gas fraction follows from the gas chord lengths and the total foam height. The gas fraction is equal to the sum of the chord lengths corresponding to the gas phase divided by the foam height. This theory is known as Rosiwal's "linear integration" (Weibel 1979). From these experiments, the conclusion could be drawn that the optimum combination of the sensor speed and the sampling rate was respectively  $10 \text{ cm s}^{-1}$  and  $1 \text{ MHz}$ . The maximum difference between the two independent calculated gas fractions was  $\pm 0.2\%$  of gas. This maximum difference includes the errors made in the measurement of the heights of the foam liquid interface and especially the foam surface. These interfaces are not completely flat. Measurements with lower sensor speeds and/or lower sampling rates resulted in differences between the gas fractions up to  $30\%$  of gas. It would be interesting to do measurements using higher sampling rates in combination with higher sensor speeds, but at this moment there is no hardware available that can measure with sample rates higher than  $1 \text{ MHz}$  and that can be used in a personal computer.

The parameters used for analysis of the signal in order to distinguish between liquid and gas were determined with experiments done with single films. Figure 2 is representing the signal when the sensor moves through a horizontal single film made in a small cylinder. From left to right, the signal corresponds to a downwards movement of the sensor. The sensor is wetted immediately when it enters the film. The signal level increases from the gas to liquid level between two sample points which corresponds to a time of  $10^{-6} \text{ s}$  ( $0.1 \mu\text{m}$  movement of the sensor) or less. When the sensor leaves the film, the signal decreases much slower to the gas level. This process takes more time because the thin liquid film that remains around the sensor tip has to drain or evaporate to a thickness of about  $0.18 \mu\text{m}$  so that a large amount of the light will be reflected in the sensor tip. Additionally there is a liquid flow in the film around the sensor tip upwards the glass fibre to the plateau border of the film that has been pierced by the sensor as a result of the higher Laplace pressure in the film at the sensor tip compared to the plateau border. The electronic noise in the signal is filtered by means of the computer program.

When the sensor is moved downwards through a foam an alternating analogue signal caused by gas and liquid phase transitions is obtained. This signal contains information about the chord lengths

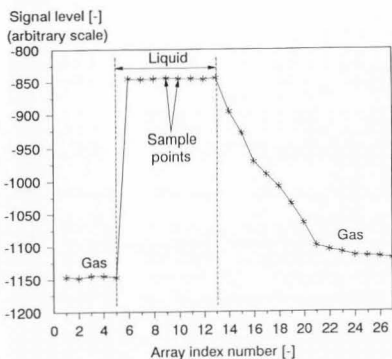


Figure 2: The signal obtained by moving the sensor through a single film.

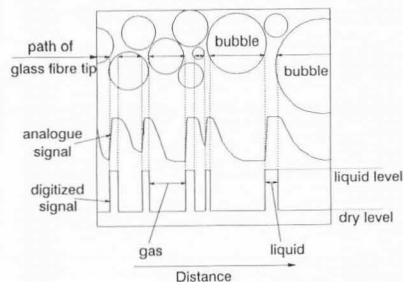


Figure 3: A schematic representation of events which occur when the sensor is moved through a foam.

the sensor travels through the phases. A schematic drawing of a part of the path of the fibre sensor through a foam is presented in figure 3. The analogue signal is sampled at 1 MHz. The data are initially stored in the internal memory of the data-acquisition board. The analogue signal is digitized by means of a computer program. The program

distinguishes between the positive and negative slopes of the analogue signal. A part of the analogue signal is considered to be "wet" (i.e. the sensor is surrounded by liquid) over the period that the slope becomes positive until it becomes negative. A part of the signal is considered to be "dry" from the moment that the slope of the signal becomes negative until it becomes positive. These parameters were chosen on the basis of results obtained from measurements of the thickness of a single lamella (see figure 2). These experiments confirmed also that the glass fibre sensor is not deteriorating the foam by moving through it. Only the mechanical part far behind the sensor tip is causing some foam collapse but it has no effect on the measurement. The sample points that are part of a "wet" signal are assigned the number 1, the "dry" sample points are assigned the number 0. This way a digital signal is obtained of which a part may look as in the next example:

```
.. 0 1 1 1 1 0 0 0 0 0 0 0 0 0 1 1 1 1 1 1 0 ..
      I           II          III
dry  wet       dry         wet  dry
```

Because the sensor speed (SS) is  $10^{-1} \text{ m s}^{-1}$  and the sampling rate (SR) is 1 MHz the distance the sensor moved between two sample points is given by  $SS/SR$  and becomes  $10^{-7} \text{ m}$ . By counting the sample points the chord lengths can be calculated. The lengths of the chords I, II and III in the example mentioned above are respectively  $0.5 \mu\text{m}$ ,  $1.0 \mu\text{m}$  and  $0.6 \mu\text{m}$ .

The chord lengths the sensor travelled through the gas phase are the basis for the calculation of the bubble-size distribution. The array of sample points has a dimension of 1,000,000. Every sample point in the array has an individual array index number. The computer program selects the array index numbers of the sample points corresponding to the liquid phase (i.e. having value 1) and stores them in a second array in the computer memory. The chord lengths can be calculated using equation 2 on the second array.

$$C_l = (N_s - N_p - 1) \cdot \left( \frac{SS}{SR} \right) \quad (2)$$

where,

- $C_l$  = The chord length [m].
- $N_s$  = The array index number of the first sample point of the subsequent "wet" chord length.
- $N_p$  = The array index number of the last sample point of the "wet" chord length preceding the "dry" chord length.
- $SS$  = Sensor speed [ $\text{m s}^{-1}$ ].
- $SR$  = Sample rate [ $\text{s}^{-1}$ ].

For the calculation of the bubble-size distribution from the gas chord lengths, a problem similar to the so called "tomato salad" problem has to be solved: The measured chord lengths of gas bubbles can not be transformed in a simple way into the actual bubble-size distribution, because the sensor hardly ever travels through the two polar ends of a bubble. Furthermore, larger bubbles have a greater chance of being pierced by the sensor than the smaller bubbles. Weibel (1980) and later Kawakami (1988) developed a statistical method to calculate the size-distribution from the chord length distribution. This method was modified and used for the calculation of the bubble-size distribution in foams. These modifications will be explained and discussed in a paper to be published in the near future. The bubble-size distribution is given as the number of bubbles per unit volume foam per class of bubble diameters. The calculated bubble diameters are assigned to 35 classes with a width of 50  $\mu\text{m}$  divided over the range from 0  $\mu\text{m}$  up to 1750  $\mu\text{m}$ .

In order to test the statistical program of the method, experiments were carried out with an almost monodisperse foam that was made by means of bubbling  $\text{N}_2$  through a capillary into a 1% Teepol solution. The diameter of the generated bubbles were varied by using capillaries with different diameters. The atmosphere above the foam was also nitrogen. Therefore gas exchange between the top layers of bubbles in the foam and the atmosphere was minimized. Nevertheless some gas diffusion out of the bubbles in the top layers to the atmosphere will take place as a result of the higher Laplace pressure in these bubbles compared to the atmospheric pressure. The number of bubbles that participate in this process is negligible compared to the total number of bubbles that are detected by the sensor in one measurement. Measurement of the bubble-size distribution in these systems showed a very narrow distributions of bubble diameters corresponding to the diameters of the generated bubbles. Figures 4a to 4c represent these bubble-size distributions of model foams with average diameters of respectively 264  $\mu\text{m}$ , 892  $\mu\text{m}$  and 1380  $\mu\text{m}$  and gas fractions of respectively 84.6%, 86.8% and 87.6%. These average diameters were determined by measuring the bubble diameters on photographs of the bubbles during generation and on photographs of the bubbles in the outer top- and side-layers of the foam. The histograms show a maximum of the number of bubbles in the class with bubble diameters corresponding with the average diameters measured on the photographs.

A routine measurement starts with pouring a fixed volume of liquid into a cylindrical glass containing a bottom of sintered glass. By moving the glass fibre downwards, the position of the liquid surface is measured and stored in the computer for use in the calculation of the gas fraction. Then a foam column is produced by dispersing gas through the glass sinter at a constant flow rate until the foam column reaches a predetermined level. In this way, a foam column of about 10 cm is produced in approximately 10 seconds. This height is necessary

to ensure that at least 500 bubbles will be detected by the sensor so that a reliable statistical calculation can be performed. The measurement is done by moving the sensor downwards through the foam in 1 second. The computer subsequently registers the upper level of the foam, the liquid-gas transitions in the foam and the position of the liquid-foam interface.

Measurements carried out in the same sample at consecutive time intervals but at different places in the same sample give information about the rate of drainage, the rate of foam collapse, the changes in foam height, foam volume and gas fraction and the evolution of the bubble-size distribution.

The Foam Analyzer has some disadvantages: (1) bubbles with a diameter smaller than the diameter of the sensor tip (i.e. 20  $\mu\text{m}$ ) are not detected or not detected in the right way. Because these small bubbles have a low contribution to the gas volume, the control of the gas fraction is not conclusive with respect to these bubbles. However, these missing bubbles (<20  $\mu\text{m}$ ) are certainly important for the foam behaviour. They promote disproportionation and if coalescence takes place the number of bubbles in the class with the smallest detectable bubbles will also increase. (2) The theory assumes that the bubbles are all of a spherical shape and are randomly distributed over the available volume which is perhaps not always the case. However, the deviation between the spherical and the polyhedral shape is not significant because the differences in the measured chord lengths will be compensated. (3) In the original bubble-size distributions, some bubble sizes are missing. This is a result of the size distribution of the holes in the glass sinter. (4) If there are changes taking place in the foam within the calculation time of the computer (i.e. one minute), only the effect of these changes after one minute can be measured. In the case of a  $\text{CO}_2$  foam disproportionation proceeds very fast, especially in the first minute. The advantages of the method are: (1) The calculation of the bubble-size distribution can be carried out within one minute: the distribution is plotted as a histogram on the computer's monitor. (2) In addition to the bubble-size distribution the rate of drainage, the rate of foam collapse, the gas fraction and the foam height can be measured in the same sample. (3) From repeated measurements, it was found that the reproducibility of the method is good.

The standard deviations of respectively drainage, collapse, foam height, gas fraction and bubble-size distribution are 0.8 mm, 0.8 mm, 1 mm, 0.5 % and 0.1 % in classes of bubbles with small diameters and 5 % in classes of bubbles with large diameters.

Although the mechanisms determining the events that occur when the sensor enters a film are not exactly known, the results of the experiments mentioned above confirm that the method gives up to a large extent accurate information about the bubble-size distribution and other physical processes that occur in the foam during ageing.

## Determination of bubble-size distributions in foams

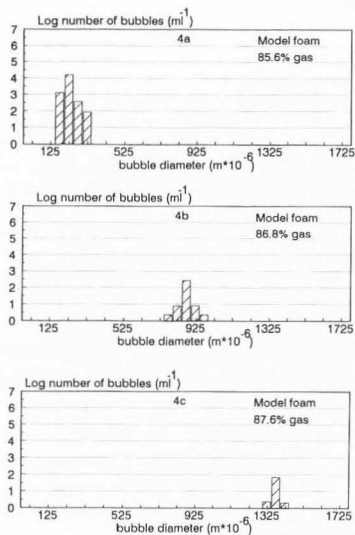


Figure 4a to 4c: The bubble-size distributions measured in model foams.

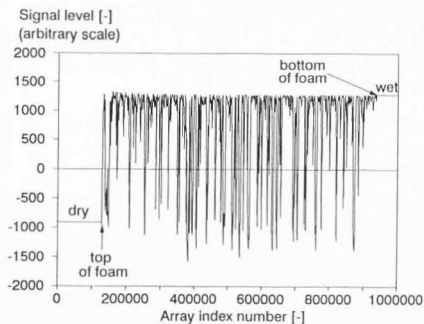


Figure 5: A typical signal obtained when moving the sensor downwards through a  $\text{CO}_2$ -foam.

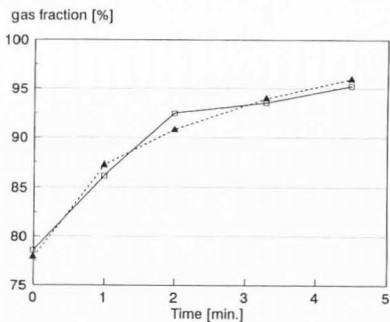


Figure 6: The measured ( $\square$ ) and the calculated ( $\blacktriangle$ ) gas fractions versus time [min.].

## Results

In figure 5, a typical signal obtained on a measurement in a  $\text{CO}_2$  beer foam is presented. For the sake of clarity, every 100th sample point of the total 1,000,000 sample points are plotted. Therefore it is a rough representation of the original signal. The signal starts at a constant low level because the sensor travels initially in air. When the sensor enters the foam, the signal increases. The position of this first gas-liquid transition is stored to calculate the foam height and gas fraction. The alternating signal of high and low values reflects the consecutive liquid-gas and gas-liquid transitions. Finally the signal remains at a constant high level at the moment the sensor passes the bottom of the foam and is travelling in liquid. The position of this foam-liquid interface is also stored for the calculation of the foam height and the gas fraction. Additionally, from the shifts in the positions of the foam surface and foam-liquid interface with time, the rate of respectively foam collapse and the rate of drainage can be calculated.

Figure 6 represents the gas fraction determined with the two independent methods mentioned above as a function of time after the production of the foam column. The standard deviations of the measured and the calculated gas fractions were  $\pm 0.48\%$  and  $\pm 0.36\%$  respectively. There are no significant differences between these gas fractions which is an argument in favour of the present technique. Repeated experiments done with foams made by using glass sinters with different pore sizes showed a very good reproducibility, even

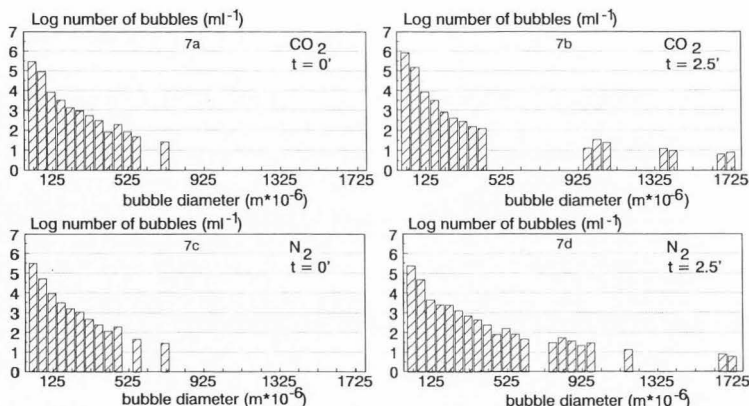


Figure 7a to 7d: The bubble-size distributions of a CO<sub>2</sub> beer foam at t=0 minutes (7a) and t=2.5 minutes (7b) and a N<sub>2</sub> beer foam at t=0 minutes (7c) and t=2.5 minutes (7d).

in foams with rather small bubbles (100-300 μm). A disadvantage is the limitation of detecting the very small bubbles as a result of the sensor diameter and the low contribution of the bubbles with small diameters to the total gas fraction in the foam. As a result there will be an error in the measurement. Compared to the expected Gaussian-shaped size distribution normally found there should be bubbles smaller than the diameter of the sensor tip. At this moment a method is being developed to produce smaller but still rigid sensor tips in order to be able to detect bubbles smaller than 20 μm.

In figures 7a and 7b, typical examples of the bubble-size distributions in a beer foam made with CO<sub>2</sub> are presented. The vertical axis is the logarithm of the number of bubbles per ml foam. Because of the logarithmic scale, small variations in bar height represent large differences in the number of bubbles. The horizontal axis is the bubble diameter distributed over classes with widths of 50 μm. The time interval between the measurements is 2.5 minutes. Additionally, the bubble-size distributions in a N<sub>2</sub>-foam of beer at t=0 minutes and t=2.5 minutes are presented in respectively the figures 7c and 7d. Initially the bubble-size distribution in a fresh foam is independent on the kind of gas that is used to produce the foam column: the bubble-size distributions in the figures 7a and 7c are approximately equal. The properties of the glass sinter in the bottom of the glass and the used liquid determine the bubble-size distribution in the initial foam column which means that gaps are found in the initial bubble-size distribution. During

ageing of the foam, the evolution of the bubble-size distribution is found to be very reproducible. In the CO<sub>2</sub>-foam and the N<sub>2</sub>-foam, the gas fractions were respectively 82.6% and 83.6%. After 2.5 minutes the gas fractions have increased to respectively 95.7% and 96.2% as the result of drainage. The bubble-size distributions of the CO<sub>2</sub>-foam and the N<sub>2</sub>-foam are now however completely different. An increase of the number of bubbles in the regions with smaller and larger diameters and a decrease of the number of bubbles in the middle region of the bubble-size distribution is an indication for disproportionation as the main physical process resulting in coarsening of the foam during ageing. These changes in the bubble-size distribution are found in the CO<sub>2</sub>-foam in which a large number of bubbles becomes smaller as can be seen most clearly in the classes with bubble diameters of 20 μm up to 75 μm. The number of bubbles in the middle region of the bubble-size distribution (450 μm-750 μm) decreases and the number of bubbles in the region with large diameters increases within the time interval of 2.5 minutes. A decrease of the number of bubbles with small diameters and an increase of the number of large bubbles and during ageing of the foam indicates that coalescence is the main physical process that leads to the breakdown of the foam. In the case of N<sub>2</sub>-foam, the number of bubbles in the region with smaller diameters (25 μm-450 μm) decreased and the number of bubbles in the region with larger diameters (750 μm-1750 μm) increased within the time interval of 2.5 minutes. Therefore

coalescence is the main physical process in  $N_2$ -foam leading to the breakdown of the foam. As a result of the 50 times higher solubility of  $CO_2$  compared to  $N_2$ , interbubble gas diffusion does take place to a large extent in the  $CO_2$ -foam within 2.5 minutes. Thus by using gasses with different solubilities, the physical processes of coalescence and disproportionation can be distinguished by measuring the bubble-size distributions.

The method can be used for different kinds of foam with the restriction that there are no hard structures in the foam that could break the very thin glass fibre. If the sample is too sticky it can foul the glass fibre sensor resulting in an inaccurate measurement (Akkerman et al. 1991).

### Conclusions

The Foam Analyzer can be used to study important physical properties of liquid foams. These properties depend to a large extent on the distribution of the gas and the liquid phase. Therefore, by measuring the bubble-size distribution in addition to the gas fraction, the rate of drainage and the rate of foam collapse, a great part of the behaviour of foams can be analyzed. The knowledge of the bubble-size distribution and gas fraction is a great advantage in the study of coalescence, disproportionation and drainage in foams.

### Acknowledgement

The authors wish to express their thanks to Eureka and the Stichting J. Mesdagfonds for their financial support. We wish to thank P. Walstra who took part in discussing this manuscript.

### References

- Akkerman JC, Bisperink CGJ, Ronteltap AD (1992). A moving optical fibre technique for structure analysis of heterogeneous products: Application to different foodstuffs. *Food Structure*, 11, 109-113.
- Frijlink JJ, (1987). Physical Aspects of Gassed Suspension Reactors. Ph.D. Diss., Technical University, Delft, The Netherlands.
- Kawakami M, Tomimoto N, Kotazawa Y, Ito K (1988). Estimation of size distribution in iron melt from the chord length distribution. *Trans. Iron. Steel. Inst. Jpn.* 28(4) pp 271-277.
- Ronteltap AD, Prins A (1989). Contribution of Drainage, Coalescence, and Disproportionation to the Stability of Aerated Foodstuffs and the Consequences for the Bubble Size Distribution as Measured by a Newly Developed Optical Glass-fibre Technique. In: *Food Colloids*, Bee RD, Richmond P, Mingsins J (eds), Royal Society of Chemistry U.K., pp 39-47.
- Ronteltap AD (1989). Beer Foam Physics. Ph.D. Diss., Agricultural University, Wageningen, The Netherlands.
- Weibel ER (1979). Stereological methods. Vol. 1, Academic Press N.Y. London, pp 27.
- Weibel ER (1980). Stereological methods. Vol. 2, Academic Press N.Y. London, pp 215.

### Discussions with Reviewers

**M. Rosenberg:** What will be the effect of other dispersed phase - fat, ice crystals?

**Answer:** The applicability to measure bubble-size distributions in systems containing fat or ice crystals was not tested. The method presented here is only applicable to liquid foams as for instance soap froth and beer foam. It has to be mentioned that the statistics used to calculate the bubble-size distribution is only applicable to systems with spherical bubbles as can be found in for instance chocomousse or beer foam.

**M. Rosenberg:** The method seems to be applicable to systems with relatively large air cells. Many food systems contain smaller air cells. In such systems, the applicability seems to be limited.

**Authors:** The limit of the bubble radius that can be detected depends on the diameter of the sensor. At this moment, a method is being developed to produce sensor tips with a diameter of 1  $\mu\text{m}$  or smaller at the end of the glass fibre. The problem is that such small sensors become very fragile and therefore have to be supported. With smaller sensors, it is possible to measure smaller bubbles.

**F. van Voorst Vader:** Figure 4 indicates that very high gas fractions were present in some samples (up to 95%). Is it still allowed to apply the "tomato salad" statistics under these conditions, or is the foam lamellar so that the statistics for cellular materials must be used?

**Authors:** The very high gas fractions are not primarily the result of a polyhedral structure but also of the heterodispersity of the foam in which the smaller bubbles are situated in the plateau borders of the larger ones. This can be illustrated by means of a simple calculation. Assuming the model presented in figure 8 with bubbles of radius R, the maximum radius of bubbles that can fit in the plateau border is described by equation 3.

$$r = R \left( \frac{2 - \sqrt{3}}{\sqrt{3}} \right) \quad (3)$$

where, R = Radii of the larger bubbles [m].  
r = Radii of the bubbles that fit in the plateau border [m].

Table 1. The maximum radii r [ $\mu\text{m}$ ] of bubbles that can fit in the plateau borders of bubbles with radii R [ $\mu\text{m}$ ].

R	1025	875	725	575	425	275	125
r	159	135	112	89	66	43	19



Table 1 shows that  $R:r$  is about 6.5:1. Therefore the smaller bubbles easily fit in the plateau borders of the larger ones that are measured and presented in the histograms in the figures 7a to 7d. Furthermore, in the plateau borders that exist in the situation presented in figure 8 can again give room to even smaller bubbles. Additionally, the three dimensional intersections of plateau borders are even larger and give more room to bubbles with smaller diameters. It can be concluded that the wider the bubble-size distribution the more possibilities there are that smaller bubbles in the distribution can fit into the plateau borders of the larger ones. The situation presented in figure 8 is a very simple assumption but it already indicates that a foam can have a very high gas fraction when the foam consists of spherical bubbles.

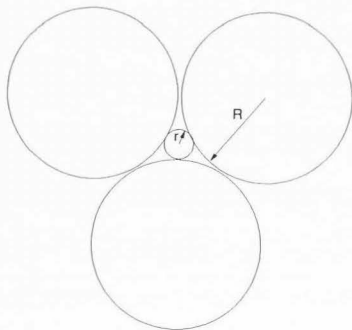


Figure 8. A schematic drawing of the plateau border between bubbles with radii  $R$  and the bubble with radius  $r$  that fits in this plateau border.

**F. van Voorst Vader:** Even droplets somewhat larger than the tip might be pushed away laterally or be entrained by its motion; this would cause errors in the measurement of the film thickness. Can you give a more extensive discussion of the interaction between the tip and the bubbles?

**Authors:** The foam has a certain stiffness. Therefore bubbles with rather small diameters can be measured and are not pushed aside by the sensor. On the other hand, small bubbles that do not take part of the stiff foam structure can be pushed aside by the sensor. To avoid this phenomenon, the first measurement is done 5 seconds after the foam column is produced. The major part of the foam column has then become dry enough as a result of drainage that leads to a stiff structure. Additionally the very small bubbles had time to rise in the plateau

borders. The plateau borders become smaller at higher levels in the foam. At a certain level, the plateau borders are so small that the rising bubbles can not move through and they are forced to take part in the rigid foam structure. The indication that the major part of the bubbles take part in the stiff foam structure is that the total number of detected bubbles does not increase between the first two measurements. Normally the first measurement 500 to 550 bubbles are detected and the second measurement 475 to 525 bubbles. An additional check are the independently determined gas fractions that have to be equal within the range of  $\pm 0.2\%$ . If these gas fractions differ by more than  $\pm 0.2\%$ , the measurement is not accepted.

**F. van Voorst Vader:** A comparison between the data obtained by the present method with those from alternative methods, using either beer foam or (preferably) stable foams would be valuable.

**Authors:** Until now no alternative method is presented in literature that can be used to compare with the data presented in this paper. The known methods have a resolution that is too low or the preparations of the sample before a measurement can be done are so radical resulting in deterioration of the foam that these methods do not give an accurate impression of the bubble-size distribution in a foam.